RESEARCH PAPER

Plant Signaling & Behavior 9, e29134; May; © 2014 Landes Bioscience

Phosphothreonine 218 is required for the function of SR45.1 in regulating flower petal development in *Arabidopsis*

Xiao-Ning Zhang[1,*], Cecilia Mo[1], Wesley M Garrett[2], and Bret Cooper[3]

[1]Department of Biology; Saint Bonaventure University; Saint Bonaventure, NY USA; [2]Animal Biosciences and Biotechnology Laboratory; USDA-ARS; Beltsville, MD USA; [3]Soybean Genomics and Improvement Laboratory; USDA-ARS; Beltsville, MD USA

Keywords: Co-immunoprecipitation, flower petal development, protein phosphorylation, regulation of RNA splicing, U5 small nuclear ribonucleoprotein

Abbreviations: Co-IP, co-immunoprecipitation; RNPS1, RNA-binding protein with serine-rich domain 1; SR45: Arginine/Serine-rich 45; U5 snRNP, U5 small nuclear ribonucleoprotein

RNA splicing is crucial to the production of mature mRNAs (mRNA). In *Arabidopsis thaliana*, the protein Arginine/Serine-rich 45 (SR45) acts as an RNA splicing activator and initiates the spliceosome assembly. *SR45* is alternatively spliced into 2 isoforms. Isoform 1 (*SR45.1*) plays an important role in the flower petal development whereas isoform 2 (*SR45.2*) is important for root growth. In this study, we used immunoprecipitation to isolate an SR45.1-GFP fusion protein from transgenic plants complementing a null mutant, *sr45–1*. Mass spectrometry suggested a single phosphorylation event in a peptide from the alternatively spliced region unique to SR45.1. Substituting alanine for threonine 218, a candidate site for phosphorylation, did not complement the *sr45–1* mutant with narrow flower petals whereas substituting aspartic acid or glutamic acid for threonine 218 did complement the *sr45–1* mutant. Mass spectrometry also revealed that other proteins involved in the spliceosome co-precipitated with SR45.1, and RT-qPCR revealed that phosphorylation of threonine 218 promotes the function of SR45.1 in promoting the constitutive splicing of *SR30* mRNA. This is the first demonstration of a specific phosphorylation site that differentially regulates the function of a plant splicing activator in physiologically and morphologically distinct plant tissues.

Introduction

In eukaryotic cells, precursor mRNAs contain both introns and exons. The spliceosome recognizes and removes intronic sequences, joining exons together to form mature mRNAs. Many proteins act in concert to fine-tune the regulation of splicing and the viability of RNA transcripts. Before being used as templates for translation, mRNAs are subjected to "quality examinations" by a conserved protein complex called the exon-exon junction complex (EJC). Four proteins, Mago, Y14, eIF4AIII and BTZ, form the EJC core, and other peripheral proteins like RNPS1 and UPFs associate with the EJC core proteins temporally. RNPS1 was originally discovered as a splicing activator in HeLa cells.[1] It couples with the UPF complex to trigger nonsense-mediated decay.[2,3] This makes RNPS1 a gateway to the RNA quality control machinery. More interestingly, RNPS1 also interacts with spliceosome components.[4-6] It is likely that RNPS1 plays an important role when the spliceosome recruits the EJC to exon junctions for the quality examination of bound transcripts. Although the discovery of alternative splicing events in eukaryotes has dramatically advanced in recent years,[7,8] the regulation mechanism in RNA splicing still remains a mystery.

In *Arabidopsis,* the sole ortholog of RNPS1 is SR45.[9] A null *Arabidopsis* mutant, *sr45–1*, exhibits pleotropic alterations to normal growth and development including delayed root growth, narrower leaves and flower petals, late flowering, and unusual numbers of floral organs.[10] In addition, *sr45–1* is hypersensitive to both ABA and glucose,[11] suggesting that SR45 not only regulates the splicing of genes that are involved in plant growth and development, but also targets a set of genes that respond to environmental changes. A recent study of *Arabidopsis* identified an SR45-binding sequence close to 5′ splice site in the 10th intron of *SR30 in vitro*. It was hypothesized that SR45 binds to this intronic sequence to recruit U1–70K and U2AF during splicing initiation.[6]

In *Arabidopsis*, *SR45* is alternatively spliced, which results in the translation of 2 different protein isoforms, SR45.1 and SR45.2. These isoforms play different roles during plant growth and development. SR45.1 helps regulate flower petal development, while SR45.2 plays a role in regulating root growth.[9]

*Correspondence to: Xiao-Ning Zhang; Email: xzhang@sbu.edu
Submitted: 03/13/2014; Revised: 05/05/2014; Accepted: 05/06/2014; Published Online: 05/15/2014
Citation: Zhang XN, Mo C, Garrett WM, Cooper B. Phosphothreonine 218 is required for the function of SR45.1 in regulating flower petal development in Arabidopsis. Plant Signaling & Behavior 2014; 9:e29134; PMID: 24832081; http://dx.doi.org/10.4161/psb.29134

This suggests that controls for the alternatively spliced SR45 isoforms are distinct with respect to plant growth and development. The SR45.1 protein isoform contains 7 extra amino acids (TSPQRKTG in place of R) compared with the SR45.2 isoform. The threonine (T) at position 218 and serine (S) at position 219 within the alternative segment in SR45.1 imply the potential for phosphorylation. Site-directed mutagenesis that converted S^{219} to alanine (A^{219} substitution) conferred no noticeable adverse effects on flower development.[9] To date, it is still unclear whether a posttranslational modification on this alternative segment correlates to the functional difference between the 2 isoforms. Nevertheless, the potential of phosphorylation control of T^{218} remains a possibility.

Little is known about the regulatory network of proteins for RNA splicing in plants. Previous in vitro studies have isolated potential SR45-interacting proteins: a splicing factor, SCL33, and spliceosomal proteins U1–70k and U2AF.[35,5,6,12] This suggests an interaction between SR45 and an SR protein and the involvement of SR45 in the initial assembly of spliceosome on pre-mRNA. Although these crucial findings advanced our understanding in how SR45 may modulate a splicing event, a lack of recognition for splicing regulation complexes hinders the mechanistic understanding of how RNA splicing is regulated in vivo.

In this study, we provide physical and phenotypic evidence for phosphorylation at SR45.1 amino acid T^{218}. More interestingly, we identified proteins that co-precipitate with phosphorylated SR45.1 in vivo. These findings suggest that there may be a stable protein network associated with SR45 in the regulation of RNA splicing in plants.

Results

Phosphorylation of SR45.1

Transgenic plants expressing SR45.1 fused to GFP were made by transformation of *sr45–1* mutants and 2 independent lines, *OX1–1* and *OX1–9*,[9] were evaluated. Inflorescence was harvested and proteins were extracted from nuclei. Anti-GFP antibody was used to precipitate SR45.1-GFP from *OX1–1* and *OX1–9*; *sr45–1* was treated similarly as a negative control. Precipitated proteins were separated by SDS-PAGE and stained. The expected mass for SR45.1-GFP fusion protein is approximately 75 kDa, and a protein band distinct to *OX1–1* and *OX1–9* samples, but not the *sr45–1* sample, migrated between the 75 kDa and 110 kDa molecular weight markers (**Fig. 1A**). The band was excised and prepared for mass spectrometry analysis. A separate gel slice at an equivalent location from the *sr45–1* sample was used as a negative control.

SR45 is arginine-rich, so trypsin was not used for digestion. Instead, proteins were digested at lysine residues using Lys-C protease. Using an Orbitrap-LTQ mass spectrometer, peptides for SR45.1-GFP were identified in *OX1–1* and *OX1–9* samples, but not in *sr45–1* samples (**Table 1**). These data confirmed that *OX1–1* and *OX1–9* were transgenic, that SR45.1-GFP could be isolated from flower nuclei, and that the presumed extracted band was SR45.1-GFP.

Lys-C digestion of SR45.1-GFP yields the diagnostic peptide, DGGPRRPRET SPQRK, which includes T^{218} and S^{219} for determining phosphorylation for isoform SR45.1. This peptide, either in the phosphorylated form or the non-phosphorylated form, was not identified using the Orbitrap-LTQ. There are many reasons for this including electron-spray ionization efficiency for the peptide and random-sampling effects associated with operating the instrument in a data-dependent manner.[13,14] Thus, another mass spectrometry method, MALDI-TOF-TOF, was used, and the instrument was operated in manual mode to scan the TOF mass spectrum for evidence of DGGPRRPRET SPQRK phosphorylation. The expected precursor *m/z* for the nonphosphorylated form of DGGPRRPRET SPQRK is 1737 (+1), whereas the expected precursor *m/z* of the singly phosphorylated form is 1817 (+1). In the *OX1–1* and *OX1–9* samples, the 1817 *m/z* peak, but not the 1737 *m/z* peak, was readily detected (**Fig. 1B**). The mass precision indicated that there was only one phosphate moiety per peptide. TOF-TOF analysis of the 1817 *m/z* peak resulted in poor *b-y* ion fragmentation and a low Mascot score, so the precise site of phosphorylation could not be determined (**Table 1** and **Fig. 1C**). Poor *b-y* ion fragmentation is a common result of MALDI-TOF-TOF-analyzed +1 charged phosphopeptides which often exhibit a primary, –98 Da phosphoric acid neutral loss peak.[15-17] As evidenced, the MALDI TOF-TOF tandem mass spectrum of the 1817 *m/z* ion exhibited a major neutral loss peak at 1719 *m/z,* which corroborates phosphorylation of DGGPRRPRET SPQRK (**Fig. 1C**). Together, these results indicate that SR45.1 is phosphorylated at either T^{218} and S^{219} in flowers.

In addition to phosphorylated DGGPRRPRET SPQRK, a phosphorylated form of VSSPPKPVSA APK was identified in SR45.1 (**Table 1**). This peptide sequence exists in both SR45 isoforms and resides in the region between the RNA recognition motif (RRM) and the C-terminal RS/SPXR domain near the spliced variant peptide DGGPRRPRET SPQRK (**Fig. 1D**). Poor *b-y* ion fragmentation prevented the determination of the amino acid positioning of the phosphate moiety, but these results suggest that SR45 is subject to phosphorylation in multiple regions.

Phosphothreonine^{218} in the SR45.1 functions in flower petal development

In a previous study, the alanine substitution for S^{219} (A^{219}) in SR45.1 did not affect petal development.[9] This suggested that either S^{219} is unlikely to be modified or it is not essential for the distinct function of SR45.1. But with respect to the mass spectrometry data, it can be deduced that T^{218} is the candidate site for phosphorylation. To test if there is a correlation between phosphorylation on T^{218} and SR45.1 activity during flower petal development, we made transgenic plants overexpressing SR45.1^{A218}, SR45.1^{D218}, or SR45.1^{E218} fused to GFP in the *sr45–1* background (**Fig. 2A, B**). SR45.1^{A218}-GFP (*T218A*) plants that had lost the capacity for phosphorylation on amino acid 218 had reduced petal width-to-length ratios similar to control transgenic plants expressing isoform SR45.2-GFP (*OX2*; **Fig. 2C**), and both sets of plants had flower petals that were significantly narrower (ratio than 80% of Col) than non-transgenic wild type plants. By contrast, SR45.1^{D218}-GFP

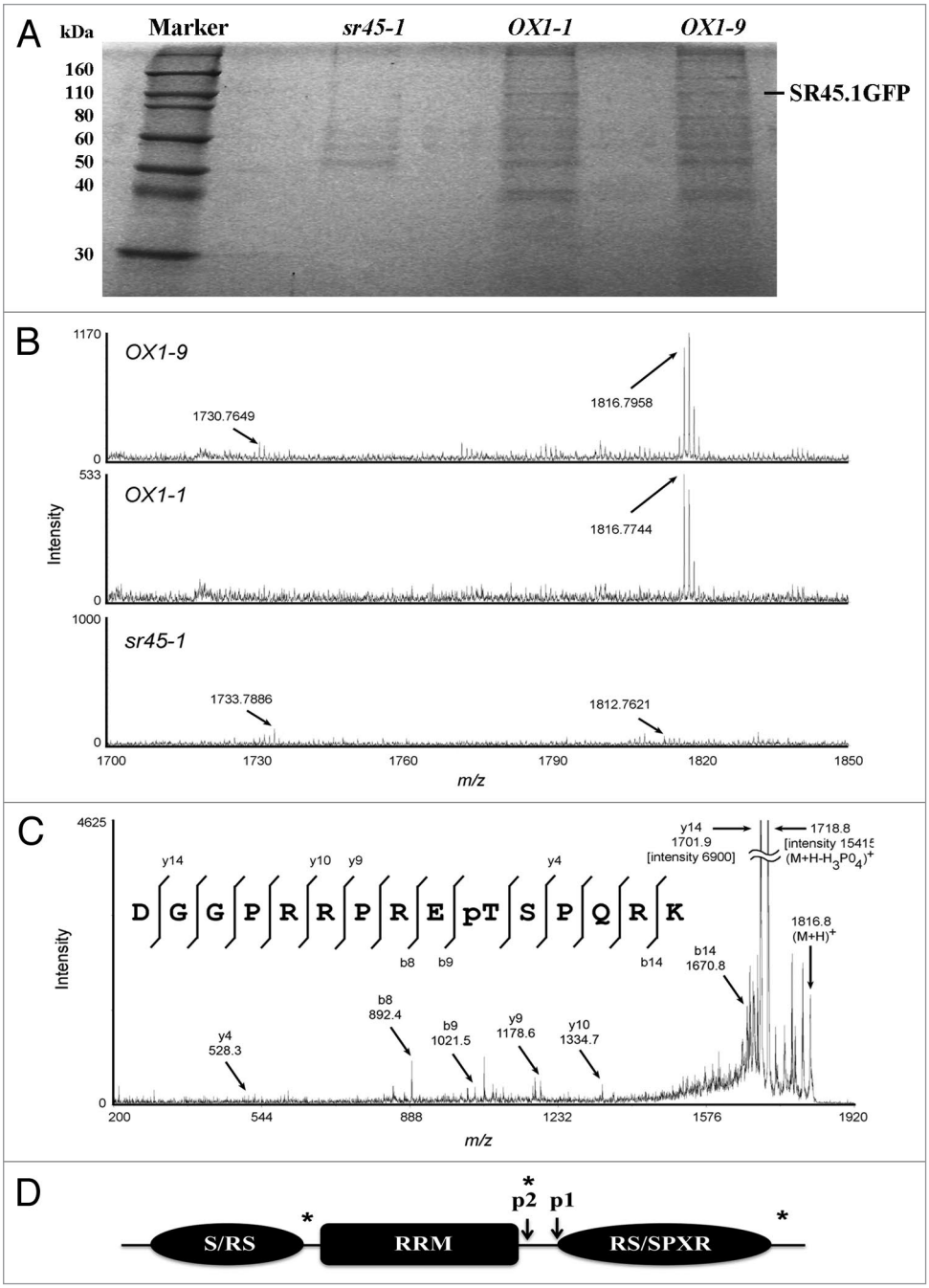

Figure 1. Mass spectrometry analysis of SR45.1-GFP peptides. (**A**) SDS-PAGE showing the protein products from immunoprecipitation. (**B**) TOF *m/z* spectrum of peptides from (**A**). The 1816.7958 and 1816.7744 *m/z* peaks are for the $(M+H)^+$ ion of phosphorylated DGGPRRPRETSPQRK. Notice the absence of the ion for the non-phosphorylated analog which would theoretically be at 1737 *m/z*. (**C**) Annotated tandem mass spectrum of phosphorylated DGGPRRPRETSPQRK. The observed *m/z* of the $(M+H)^+$ ion is 1816.83. The *m/z* for the phosphoric acid neutral loss ion is 1718.8 and is the dominant peak in the spectrum. (**D**) Protein domain structure showing the phosphorylation sites in SR45.1 identified by mass spectrometry. Phosphorylation sites, p1 from (**C**) and p2 identified in this study are indicated by arrows. Phosphorylation sites identified by previous studies[19,20] are indicated by *.

(*T218D*) and SR45.1^{E218}-GFP (*T218E*) plants containing a negatively charged carboxyl group that can mimic the effect of phosphothreonine had petal width-to-length ratios greater than the alanine mutant (*T218A*) and similar to *OX1* positive controls. The petal width-to-length ratios of *T218D, T218E* and *OX1* plants were restored to 85–90% of those for non-transgenic wild-type plants (**Fig. 2C**). These results suggest that phosphorylation at T^{218} is important for the function of SR45.1 in flower development and that substitution of a negative charge at this position can restore the distinct function.

Regulation of the alternative splicing of *SR30* by T218 phosphomimics

Studies have shown that SR45.1 directly binds to intron 10 of *SR30* pre-mRNA in vitro,[6] and the alternative splicing pattern of

Table 1. Proteins and peptides identified by tandem mass spectrometry and database search

Inflorescence	Protein	mol wt.	Gel 1 position	Gel 2 position	Gel 3 position	peptides	Mascot Ions score	Mascot Expect	Instrument
OX1–1, OX1–9	MEE5 (AT1G06220)	111 kDa	N.E.	~130 kDa	~130 kDa	K.IYSQVIGEHKK	40	0.01	MALDI
						K.DLRELYSEVEVK	72	5.60E-06	MALDI
						K.AVPMSLVLEDSRSK	49	1.40E-03	MALDI/Orbitrap
						K.CFAETPNK	44	1.80E-04	Orbitrap
						K.TATEPLNPSELPK	60	6.30E-06	Orbitrap
						K.YTDTRVDEQERNISIK	57	2.20E-04	MALDI
OX1–1, OX1–9	SR45.1GFP	72.5 kDa	~80 kDa	~80 kDa	~80 kDa	K.RHDFFK	35	2.30E-02	MALDI/Orbitrap
						K.ATFTLPPRQK	41	7.10E-03	MALDI/Orbitrap
						K.FSVSGEGEGDATYGK	79	7.60E-07	MALDI/Orbitrap
						K.FEGDTLVNRIELK	54	4.20E-04	MALDI
						K.GIDFKEDGNILGHK	51	7.70E-04	MALDI
						K.DGGPRRPREpTSPQRK	18	1.7	MALDI
						K.DGGPRRPRETpSPQRK	22	0.76	MALDI
						K.AQLYMDGAQIDGK	94	5.50E-09	MALDI/Orbitrap
						K.VSpSPPKPVSAAPK	22	6.90E-02	Orbitrap
						K.TRAEVKFEGDTLVNRIELK	35	3.70E-02	MALDI
						K.SAMPEGYVQERTIFFK	36	2.40E-02	MALDI
OX1–1, OX1–9	SR34a (AT3G49430)	33.8 kDa	N.E.	~38 kDa	~38 kDa	K.YGRIVDIELK	49	1.10E-03	MALDI/Orbitrap
OX1–1, OX1–9	transducin (AT2G43770)	38.3 kDa	N.E.	~38 kDa	~38 kDa	K.TVRAWDVETGK	33	2.40E-02	MALDI/Orbitrap
						K.IFEGHQHNFEK	50	5.70E-04	MALDI
						K.YQITAVSFSDAADK	74	2.40E-06	MALDI
						K.NIYLGEI	37	2.10E-03	Orbitrap
						K.IFTGGVDNDVK	47	2.40E-04	Orbitrap
OX1–1, OX1–9	transducin (AT1G10580)	65.7 kDa	N.E.	N.F.	~80 kDa	K.GVSAIRFFPK	38	6.70E-03	MALDI
						K.DYQGRSWIEAPK	31	5.60E-02	MALDI
						K.FLTAGYDK	26	1.80E-02	Orbitrap
						K.QNILLAGoxMSDK	28	1.90E-02	Orbitrap
						K.EVVQGELTEEQK	75	3.70E-07	Orbitrap
OX1–1, OX1–9	SCL33 (AT1G55310)	25.5 kDa	N.E.	~38 kDa	~38 kDa	K.SFEQFGPVK	60	4.70E-05	MALDI
OX1–9	SR34 (AT1G02840)	33.8 kDa	N.E.	N.F.	~38 kDa	K.YGPVVQIDLK	55	1.20E-04	MALDI/Orbitrap
OX1–1, OX1–9	RSZ21 (AT1G23860)	21.7 kDa	N.E.	N.F.	~24 kDa	K.NGWRVELSHK	39	6.60E-03	MALDI

Lower case "p" preceding an amino acid indicates phosphorylation on that amino acid; lowercase "ox" preceding an amino acid indicates oxidation on that amino acid. N.E. = not examined.

SR30 is correlated with flower petal development.[9] Therefore, we tested if phosphorylation of SR45.1 affects the splicing pattern of *SR30* using reverse transcription-quantitative PCR (RT-qPCR). We examined the ratios of the 2 alternatively spliced isoforms of *SR30* pre-mRNA, isoform 1 (*SR30.1*) and isoform 5 (*SR30.5*) in inflorescence (**Fig. 3A**). *SR30* intron 10 is constitutively spliced in *SR30.1*, while a proximal alternative 3′ splice site is used in *SR30.5* which introduces a premature termination codon. In wild type inflorescence, *SR30.1* is the dominant isoform which yielded a low ratio of *SR30.5/SR30.1* (**Fig. 3B**). Low ratios of *SR30.5/SR30.1* were also observed in *OX1*, *T218D* and *T218E* transgenic plants that are negatively charged at position 218 in SR45.1. By contrast, the *sr45–1* mutant exhibited a significantly higher ratio of *SR30.5/SR30.1* (**Fig. 3B**), and the *SR30.5/SR30.1* ratios in *OX2* and *T218A* transgenic plants were more similar to the higher ratio seen in the *sr45–1* (**Fig. 3B**). Since all transgenes

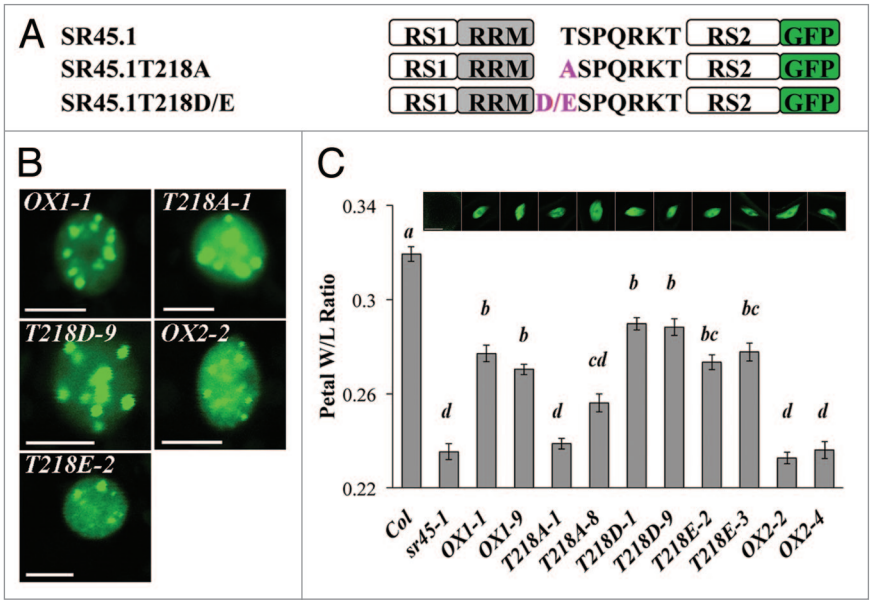

Figure 2. Amino acid substitution tests for T^{218}. (**A**) The domain structure of SR45.1-GFP and residue substitution mutant constructs. (**B**) The GFP signal was examined in the nucleus of hypocotyl cells of 4-d-old seedlings as indicated. Scale bars represent 10 μm. (**C**) Petal width-to-length (W/L) ratio of the Col wild type, *sr45–1* mutant and 2 independent lines for each transgene in the order as indicated in the figure. Error bars present standard error of the mean (SEM) from 40 flower petals. Statistically significant differences ($P < 0.001$) are indicated by letters a-d. The GFP signal was also examined in trichomes of the *sr45–1* mutant and each transgenic line. The same parameters (laser intensity = 80%, 488nm; Gain = 7.60B; Offset = 127) were used for all lines. Scale bar = 25 μm.

were expressed at a comparable level as indicated by the intensity of the GFP signal (**Fig. 2C**), it is unlikely that the difference in the alternative splicing pattern of *SR30* is due to a different abundance in SR45 protein. These data imply that the phosphorylation status at T218 modulates SR45.1 function in regulating the splicing of its direct target, intron 10 of *SR30* pre-mRNA.

Proteins associated with SR45.1

Upon repeating immuno-affinity experiments for *OX1–1* and *OX1–9* inflorescence, we noticed in addition to the SR45.1-GFP band the appearance of other bands in *OX1–1* and *OX1–9,* but not *sr45–1* samples. The additional bands implied that other proteins precipitated with SR45.1-GFP, possibly through protein-protein interactions. Maternal Effect Embryo Arrest 5 (MEE5, AT1G06220), a 111 kDa protein homologous to human U5–116kD and yeast splicing factor Snu114,[18] was found in a position above SR45.1-GFP that was consistent with its theoretical size (**Table 1**). The peptide coverage for MEE5 was similar to SR45.1-GFP which suggests that their abundances were similar. Two SR proteins, SR34a (AT3G49430) and SCL 33 (AT1G55310), and a transducing/WD40-like protein (AT2G43770) that is part of the nuclear CUL4-RING ubiquitin ligase complex migrated near molecular weight markers consistent with their smaller sizes (**Table 1**). These proteins also appeared in similar positions in a third preparative gel of proteins immuno-precipitated with SR45.1-GFP. In the third gel, another 2 SR proteins, SR34 (AT1G02840) and RSZ21 (AT1G23860), and a second, larger transducing/WD40-like protein (AT1G10580), were found. Peptide coverage was sparse for these additional splicing factors. If they associate with SR45.1-GFP, their interactions may be weaker than for MEE5. None of these proteins appeared in similar positions in *sr45–1* samples, and this corroborates the idea that these proteins specifically interacted with SR45.1-GFP as opposed to non-specifically interacted with the GFP antibody.

Discussion

We have discovered that phosphorylation of T^{218} is key to the distinct function of SR45.1 in petal development and mRNA splicing in inflorescence. This is the first demonstration of a specific phosphorylation site that regulates the function of a plant splicing activator. The transcript of SR45 encoding gene is itself a target of alternative splicing and can produce 2 protein isoforms, SR45.1 and SR45.2. SR45.1 is distinct from SR45.2 by having 7 additional amino acids (TSPQRKTG in place of R). Two of these additional residues, T^{218} and S^{219}, made us wonder whether phosphorylation influenced the specific role of SR45.1 in flower petal formation. Here we show by immunoprecipitation and mass spectrometry of GFP-tagged SR45.1 that this extended fragment of SR45.1 is phosphorylated at a single site, either T^{218} or S^{219} (**Fig. 1B, 1C**). The non-phosphorylated form of the distinguishing fragment of SR45.1 was not observed in inflorescence tissues. This implies that the distinguishing peptide in SR45.1 is mostly phosphorylated in the inflorescence. Prior work ruled out S^{219} as being essential for petal development.[9] Analysis of mutants carrying individual alanine, glutamic acid and aspartic acid substitutions presented here confirmed that T^{218} is the site of phosphorylation and that phosphorylation is required for normal petal formation (**Fig. 2**).

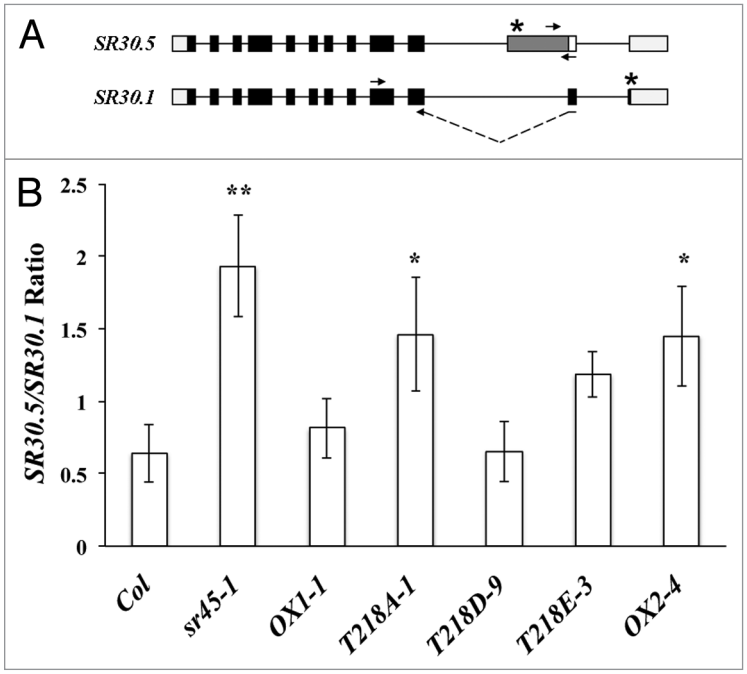

Figure 3. Alternative splicing pattern of *SR30*. (**A**) Two gene models, *SR30.1* and *SR30.5*, showing an alternative 3′splice site within intron 10 in *SR30.5*. Exons: black boxes; introns: straight lines; UTRs: white boxes; and alternative exon: gray box. Stop codons in use are indicated by *. The position of primers used for RT-qPCR are shown as arrows. (**B**) The ratio of *SR30.5/SR30.1* was examined in each genotype ($n = 3$). All ratios were compared with Col. Error bars present standard deviations. The Student *t*-test was used for statistical analysis (* $P < 0.05$; ** $P < 0.01$).

Mass spectrometry also revealed a second phosphorylation site at S^{183} (**Table 1**, **Fig. 1D**). This phosphosite resides immediately after the RRM domain and has been observed before in dark-grown root cell cultures.[19,20] Thus, this modification is neither specific to flowers nor roots, and is therefore not likely to be critical just to petal development, although it may be important for general SR45.1 activities across tissue types. Additional SR45 phosphosites identified by others (**Fig. 1D**)[19] but not observed by us may be specific to the dark-grown root cells. Therefore, we hypothesize that phosphorylated T^{218} regulates the splicing of a specific set of transcripts in flowers by SR45.1, while phosphorylated S^{182} or S^{183} may regulate the splicing of a common group of transcripts in both petal and root cells by SR45.1 and SR45.2.

Since SR45 is a versatile splicing regulator, the phosphorylation of SR45 may change its ability to identify target transcripts. Recently, SR45.1 was found to directly bind to intron 10 of *SR30* transcript in vitro.[6] Our tests show that phosphorylation of T^{218} promotes constitutive splicing to form *SR30.1* (**Fig. 3B**). This alternative splicing pattern change coincides with the change in petal development. It will be interesting to see whether SR45.1 binds to the *SR30* intronic sequence in vivo and whether the binding is tissue-specific or generic across all tissues.

SCL33 was previously shown to interact with SR45.1 in vitro,[5] and our in vivo studies confirmed this association. In addition, we found 6 other proteins that co-precipitated with SR45.1. None has been shown to interact with SR45.1 in the past. Three of the proteins are annotated as homologs of U5 snRNP proteins in other species (**Table 2**). We did not, however, find U1–70K and U2AF[35] associating with SR45.1 as have others.[5,6] Multiple explanations can explain this discrepancy: 1) the proteins we studied were isolated from live inflorescence whereas the other interactions were observed in vitro; 2) we limited our examination to visible proteins on the SDS-PAGE gels; 3) our immunoprecipitation protocol may have precluded some interactions after nuclear extraction. All the identified proteins are involved in splicing, which indicates that they are unlikely due to non-specific binding to the GFP antibody. However, we cannot completely exclude the possibility that anti-GFP antibody may cause some non-specific binding. Improvement to our immunoprecipitation methodology will help minimize the current limitations and resolve additional protein-protein interactions of the spliceosome complex. Testing protein-protein interactions with various in vitro essays will provide additional information in whether and how these proteins associate with SR45, either directly or indirectly. It is also possible that the phosphorylation of SR45 affects its interactions with other proteins in the spliceosome complex. We expect this to be a testable hypothesis using the mutants and assays we have developed.

Our results imply that SR45.1-associated U5 snRNP components include MEE5 and 2 transducins. MEE5, also known as CLO or FGA1, is a splicing factor required for female gametophyte development and embryogenesis.[18] It is homologous to Snu114, a GTPase required for spliceosome activation (also known as the formation of B* complex). This surprising finding leads to a potentially new role of SR45 in later steps of spliceosome assembly in addition to initiation. The 2 transducins associated with SR45.1 are part of the nuclear CUL4-RING

Table 2. A summary of SR45-interacting proteins

SR45 interacting proteins	Gene Locus	Spliceosome components	Detection Methods	Experimental Materials	Reference PMIDs
AFC2	At4g24740	no	protein kinase assay	cDNA library from 3D old etiolated seedlings	10593939
Cactin	At1g03910	no	flourescence imaging	4D old transgenic seedling, RAM cells	23454656
MEE5/Snu114-like (in U5 snRNP)	At1g06220	yes	Co-IP	long day grown inflorescence	This study
RNU1 (U1 70k)	At3g50670	yes	Y2H, in vitro pull down	cDNA library from 3D old etiolated seedlings	10593939
RSZ21	At1g23860	yes	Co-IP	long day grown inflorescence	This study
SCL33	At1g55310	yes	co-IP	long day grown inflorescence	This study
		yes	in vitro pull down	cDNA library from 3D old etiolated seedlings	10593939
SKIP/Prp45 (in U5 snRNP)	At1g77180	yes	FRET	Tobacco leaf	22942380
SR34	At1g02840	yes	Co-IP	long day grown inflorescence	This study
SR34a	At3g49430	yes	Co-IP	long day grown inflorescence	This study
Transducin (in U5 snRNP)	At2g43770	yes	Co-IP	long day grown inflorescence	This study
Transducin (in U5 snRNP)	At1g10580	yes	Co-IP	long day grown inflorescence	This study
U2AF35A	At1g27650	yes	BiFC	protoplasts	22563826
U2AF35B	At5g42820	yes	BiFC	protoplasts	22563826

ubiquitin ligase complex and are involved in the ubiquitin-mediated protein degradation system (UPS). It was reported that both were able to interact with SPF27/MOS4, a splicing factor that is essential for plant innate immunity.[21] Thus, it is possible that these 2 transducins may mediate the turnover of SR45.1 and/or SR45.1-associated proteins by UPS.

New roles of SR45 are emerging. A recent study shows that SR45 may also affect siRNA-mediated gene silencing.[22] This opens a new avenue for understanding how SR45 controls cellular activities. Coincidentally, a new discovery in yeast finds a genome defense mechanism with which the siRNA-mediated gene silencing pathway is in competition with RNA splicing for pre-mRNAs.[23] Experiments to determine direct RNA targets of SR45 in *Arabidopsis* will provide more insights in the regulatory function of SR45 in these crucial subcellular events.

Materials and Methods

Plant growth condition

All *Arabidopsis thaliana* plants used in this study are Colombia (Col-0). The *sr45–1* (SALK_004132) mutant was obtained from the Arabidopsis Biological Resource Center (ABRC). Primers that were used to examine T-DNA insertions were described in a previous study.[9] All plants were grown in soil with a 16/8 h photoperiod at 100 μmol m^{-2} s^{-1}. Peter's fertilizer (Griffin Greenhouse and Nursery Supplies, 67–2030) was applied once at the concentration of 3 g L^{-1} after the first week. All plants were grown at 24 °C.

RNA isolation and RT-qPCR

The RNeasy Mini Kit (Qiagen) was used to isolate total RNAs. About 5 micrograms of total RNA from each sample were used for reverse transcription with Superscript II system (Invitrogen). The alternative splicing pattern of *SR30* was examined by RT-qPCR on a Chromo4 DNA Engine Thermocycler (Bio-Rad). *GAPDH* was used as a reference control. Power SYBR Master mix (Invitrogen) was used to set up qPCR reactions. Primer sequences used were *SR30.1F:* 5′-GTG TGA GTC GAA GCC CAG AT-3′, *SR30.1R:* 5′-CTT GAT TGG GAC CTT GAG AC -3′, *SR30.5F:* 5′-TGT TTT TAC GGT CTG GTC TGG-3′, *SR30.5R*: 5′-ATT GGG ACC TGC AGC AAG A-3′, *GAPDHF:* 5′-CAA GGA GGA ATC TGA AGG CAA AAT GA-3′ and *GAPDHR:* 5′-CAA CCA CAC ACA AAC TCT CGC CG-3′. Three biological replicates were evaluated. The ratio of *SR30.5/SR30.1* was analyzed using the Livak method.[24]

Amino acid substitution

A QuikChange II XL Site-Directed Mutagenesis kit (Agilent) was used to introduce point mutations to *SR45.1*. *pBart-35S::SR45.1:GFP*, named *SR45.1*,[9] was used as the template to generate the mutation that resulted in T^{218} to A^{218} (*T218A*) with primers *SR45T218AF*: 5′- GGC GCC CAA GAG AGG CAT CTC CTC AAC GG-3′ and *SR45T218AR*: 5′- CCG TTG AGG AGA TGC CTC TCT TGG GCG CC-3′. The altered construct was then used as the template to generate mutations for T^{218} to D^{218} (*T218D*) and T^{218} to E^{218} (*T218E*) in the SR45.1 protein with primers *SR45A218DF:* 5′- GGC GCC CAA GAG AGG ACT CTC CTC AAC GGA-3′, *SR45A218DR*: 5′-TCC GTT GAG GAG AGT CCT CTC TTG GGC GCC-3′, *SR45A218EF*: 5′- GGC GCC CAA GAG AGG AAT CTC CTC AAC GGA-3′ and *SR45A218ER*: 5′- TCC GTT GAG GAG ATT CCT CTC TTG GGC GCC-3′. All sequences were confirmed by sequencing performed by Genewiz, Inc.

Plant transformation, screening and isolation of transgenic plants

DNA plasmids *T218A*, *T218D* and *T218E* were individually transformed into *Agrobacterium tumefaciens* GB3101 and used to transform *sr45–1* mutant plants by flower-dipping.[25] All T1 plants were screened for *basta* resistance when sprayed with Finale (1/1000 dilution) and examined for the GFP signal using a Nikon D-Eclipse C1 confocal microscope. At least 2 independent transgenic lines were selected for further analysis.

T3 and T4 plants that exhibited the GFP signal were used for further examinations.

Statistical analysis of petal width-to-length ratio

The software Image J (rsb.info.nih.gov/ij/) was used to determine petal width and length. A total of 40 flower petals were measured for each genotype. The Student *t*-test with Bonferroni correction was used for statistical analysis ($P < 0.001$).

Immunoprecipitation

CeLLytic™ PN Isolation/Extraction Kit (Sigma, Cat#CELLYTPN1–1KT) was used for nuclei isolation. The inflorescence tissue was harvested and immediately ground into fine powder in liquid nitrogen. About 25 mL of the fine powder was suspended thoroughly in 40 mL of 1x nucleus isolation buffer (NIB). The suspension was filtered through Miracloth and centrifuged at 1260 x *g* for 10 min. at 4 °C. NIBA solution was made by adding 1 tablet of protease inhibitors (Roche), 100 μL of phosphatase inhibitor cocktail II and 100 μL of phosphatase inhibitor cocktail III (Sigma) in 10 mL of NIB. The supernatant was discarded, and the pellet was resuspended completely in 2 mL of NIBA. 10% Triton X-100 was added to a final concentration of 0.3% to lyse the cell membrane. The lysate was centrifuged at 12,000 x *g* for 10 min. at 4 °C. The pellet was resuspended with 1 mL of NIBA and centrifuged again at 12,000 x *g* for 10 min. Then the pellet was resuspended in 0.5 mL of extraction buffer (1x IP buffer from Invitrogen, Cat#14321D with protease inhibitors, phosphatase inhibitors, 1/200 PMSF and 1mM DTT) with 20 μL of 10% SDS. Another 0.5 mL of extraction buffer was added to the suspension. The mixture was centrifuged at 12,000 x *g* for 10 min. at 4 °C. This step was repeated until the supernatant was clear. Anti-GFP antibody was coupled to Dynabeads per the manufacturer's instructions (Invitrogen). The clear supernatant was mixed with Dynabeads-GFP antibody and incubated on a rotator at 4 °C for 1 h. The beads then were washed as recommended and eluted with 2 x 200 μL of HPH EB (0.5 mM EDTA, 0.5 M NH_4OH). The elution was frozen in liquid nitrogen and lyophilized in a freeze drier.

SDS-PAGE and protein staining

The lyophilized protein sample was dissolved in 50 μL of 2x SDS loading buffer and heated at 100 °C for 5 min. All samples were loaded on a 10% SDS-PAGE gel. After electrophoresis, the gel was stained in Gelcode Blue Safe Stain (Pierce) overnight and destained in deionized water until protein bands were optimal for visualization.

Mass spectrometry

Stained protein bands were excised from the gels and destained, and the proteins were reduced and carboxyamidomethylated as previously described.[26] The proteins then were digested by Lys-C. The resulting peptides were co-crystalized with a 5 mg/ml α-cyanohydroxycinnamic acid matrix prepared in 50% acetonitrile/0.1% trifluoroacetic acid. An AB SCIEX 5800 TOF/TOF (Framingham, MA) was used to generate tandem mass spectra (MS^2). A plate model calibration of bovine serum albumin peptides was performed to optimize mass accuracy and to update the instrument's default calibration parameters. For the *A. thaliana* samples, a survey MS scan was performed and then MS^2 was manually performed on 1817 *m/z* ions. Then the instrument was operated in automatic mode to acquire MS^2 spectra on 100 of the strongest MS precursor ions. An exclusion mass list prevented MS^2 analysis of common contaminants. MS spectra were acquired in positive ion reflector mode with 400 shots of a 349 nm Nd:YAG laser operating at 404 Hz. MS^2 spectra were also acquired in positive ion reflector mode with 250–1000 laser shots firing at a rate of 1010 Hz. Collision energy was set to 1 kV and collision induced dissociation (CID) was enabled with air in the CID cell. MS^2 spectra were extracted with Mascot Distiller 2.3.2 (Matrix Science, London, UK). Sets of MS^2 spectra were searched independently with Mascot 2.4.0.[27] Search parameters were for Lys-C digests, 1 possible missed cleavage, fixed amino acid modification [+57, C], variable amino acid modifications for phosphorylation [+80, S,T] and oxidation [+16, M], monoisotopic mass values, ± 100 ppm parent ion mass tolerance, ± 0.8 Da fragment ion mass tolerance, and #13C = 1 enabled. The searched database consisted of version 8.0 of the *A. thaliana* genome protein reference database (ftp://ftp.arabidopsis.org/home/tair/Sequences/blast_datasets/; 32,825 records) appended with a list of common contaminants (32,997 records total). The database sequence for AtSR45.1 was modified to include the GFP protein sequence. Peptide-spectrum matches with Expect values less than 0.05 are considered significant, but lesser matches are shown for illustrative purposes.

The peptides were also analyzed by liquid chromatography tandem mass spectrometry (LC- MS^2). Peptides were separated on a C18 reverse phase column (100 x 0.18 mm BioBasic-18) using a linear gradient from 5% to 40% acetonitrile/0.1% formic acid at a flow rate of 3 mL/min which was controlled by an Accela HPLC pump (Thermo Fisher Scientific, Waltham, MA). The eluent was electrosprayed at 3.5 kV directly into the orifice of an LTQ-Orbitrap XL mass spectrometer[28] (Thermo Fisher Scientific) controlled by Xcalibur 2.0.7 software (Thermo Fisher Scientific). A parent-ion scan was performed in the Orbitrap over the range of 400-1600 *m/z* at 30,000 resolution, 1 000 000 automatic gain control (AGC), 750 ms ion injection time, and 1 μscan. Lock-mass was enabled.[29] Data-dependent MS^2 and MS^3 were performed in the linear ion trap with 10,000 AGC and 100 ms ion injection times with 3 μscans. MS^2 was performed on the 5 most intense MS ions, and MS^3 was triggered if one of the top 3 MS^2 ions corresponded with neutral loss of 98.0, 49.0, and 32.7 Da for +1, +2 and +3 charged ions, respectively.[30] Minimum signals were 5,000 and 500 respectively. An isolation width of 2 *m/z* and normalized collision energy of 35% were used for MS^2 and $MS.^3$ Dynamic exclusion was used with a repeat count of 1, 30 s repeat duration, a list of 50, list duration of 3 min and exclusion mass width of ± 0.7 Da. MS^2 and MS^3 spectrum data files were separately extracted from the raw data with Bioworks 3.3.1 (Thermo Fisher Scientific) using the parameters 600–4,500 mass range, 0 group scan, 1 minimum group count, and 5 minimum ion counts. Sets of MS^2 and MS^3 spectra were searched independently with Mascot 2.4.0. For MS^2 spectra, search parameters

were as above but with ± 10 ppm parent ion mass tolerance. For MS^3 spectra, search parameters were for Lys-C digests, 1 possible missed cleavage, fixed amino acid modification [+57, C], variable amino acid modifications [-18, S, T], [+80, S, T], and [+16, M], monoisotopic mass values, ± 1.5 Da parent ion mass tolerance, and ± 0.8 Da fragment ion mass tolerance.

Disclosure of Potential Conflicts of Interest

No potential conflicts of interest were disclosed.

Acknowledgments

We thank ABRC for seeds; 2 students, Jason Chien and Sinead Coleman, for their help in preparing transgenic plants; and all members in Zhang lab for their support. We also thank Dr Caren Chang for hosting the visit to her laboratory and Drs Caren Chang, Heven Sze, and Stephen Mount for their constructive comments. This work was supported by the research fund in Department of Biology at St. Bonaventure University and National Science Foundation (NSF 0950158 and NSF 1146300) grants to X.Z.

References

1. Mayeda A, Badolato J, Kobayashi R, Zhang MQ, Gardiner EM, Krainer AR. Purification and characterization of human RNPS1: a general activator of pre-mRNA splicing. EMBO J 1999; 18:4560-70; PMID:10449421; http://dx.doi.org/10.1093/emboj/18.16.4560
2. Lykke-Andersen J, Shu MD, Steitz JA. Communication of the position of exon-exon junctions to the mRNA surveillance machinery by the protein RNPS1. Science 2001; 293:1836-9
3. Palusa SG, Reddy AS. Extensive coupling of alternative splicing of pre-mRNAs of serine/arginine (SR) genes with nonsense-mediated decay. New Phytol 2010; 185:83-9; PMID:19863731; http://dx.doi.org/10.1111/j.1469-8137.2009.03065.x
4. Sakashita E, Tatsumi S, Werner D, Endo H, Mayeda A. Human RNPS1 and its associated factors: a versatile alternative pre-mRNA splicing regulator in vivo. Mol Cell Biol 2004; 24:1174-87; PMID:14729963; http://dx.doi.org/10.1128/MCB.24.3.1174-1187.2004
5. Golovkin M, Reddy AS. An SC35-like protein and a novel serine/arginine-rich protein interact with Arabidopsis U1-70K protein. J Biol Chem 1999; 274:36428-38; PMID:10593939; http://dx.doi.org/10.1074/jbc.274.51.36428
6. Day IS, Golovkin M, Palusa SG, Link A, Ali GS, Thomas J, Richardson DN, Reddy AS. Interactions of SR45, an SR-like protein, with spliceosomal proteins and an intronic sequence: insights into regulated splicing. Plant J 2012; 71:936-47; PMID:22563826; http://dx.doi.org/10.1111/j.1365-313X.2012.05042.x
7. Pan Q, Shai O, Lee LJ, Frey BJ, Blencowe BJ. Deep surveying of alternative splicing complexity in the human transcriptome by high-throughput sequencing. Nat Genet 2008; 40:1413-5; PMID:18978789; http://dx.doi.org/10.1038/ng.259
8. Marquez Y, Brown JW, Simpson C, Barta A, Kalyna M. Transcriptome survey reveals increased complexity of the alternative splicing landscape in Arabidopsis. Genome Res 2012; 22:1184-95; PMID:22391557; http://dx.doi.org/10.1101/gr.134106.111
9. Zhang XN, Mount SM. Two alternatively spliced isoforms of the Arabidopsis SR45 protein have distinct roles during normal plant development. Plant Physiol 2009; 150:1450-8; PMID:19403727; http://dx.doi.org/10.1104/pp.109.138180
10. Ali GS, Palusa SG, Golovkin M, Prasad J, Manley JL, Reddy AS. Regulation of plant developmental processes by a novel splicing factor. PLoS One 2007; 2:e471; PMID:17534421; http://dx.doi.org/10.1371/journal.pone.0000471
11. Carvalho RF, Carvalho SD, Duque P. The plant-specific SR45 protein negatively regulates glucose and ABA signaling during early seedling development in Arabidopsis. Plant Physiol 2010; 154:772-83; PMID:20699397; http://dx.doi.org/10.1104/pp.110.155523
12. Ali GS, Prasad KV, Hanumappa M, Reddy AS. Analyses of in vivo interaction and mobility of two spliceosomal proteins using FRAP and BiFC. PLoS ONE 2008; 3:e1953
13. Liu H, Sadygov RG, Yates JR 3rd. A model for random sampling and estimation of relative protein abundance in shotgun proteomics. Anal Chem 2004; 76:4193-201; PMID:15253663; http://dx.doi.org/10.1021/ac0498563
14. Cooper B, Feng J, Garrett WM. Relative, label-free protein quantitation: spectral counting error statistics from nine replicate MudPIT samples. J Am Soc Mass Spectrom 2010; 21:1534-46; PMID:20541435; http://dx.doi.org/10.1016/j.jasms.2010.05.001
15. Bennett KL, Stensballe A, Podtelejnikov AV, Moniatte M, Jensen ON. Phosphopeptide detection and sequencing by matrix-assisted laser desorption/ionization quadrupole time-of-flight tandem mass spectrometry. J Mass Spectrom 2002; 37:179-90; PMID:11857762; http://dx.doi.org/10.1002/jms.271
16. Lemeer S, Kunold E, Klaeger S, Raabe M, Towers MW, Claudes E, Arrey TN, Strupat K, Urlaub H, Kuster B. Phosphorylation site localization in peptides by MALDI MS/MS and the Mascot Delta Score. Anal Bioanal Chem 2012; 402:249-60; PMID:22038583; http://dx.doi.org/10.1007/s00216-011-5469-2
17. Palumbo AM, Reid GE. Evaluation of gas-phase rearrangement and competing fragmentation reactions on protein phosphorylation site assignment using collision induced dissociation-MS/MS and MS3. Anal Chem 2008; 80:9735-47; PMID:19012417; http://dx.doi.org/10.1021/ac801768s
18. Liu M, Yuan L, Liu NY, Shi DQ, Liu J, Yang WC. GAMETOPHYTIC FACTOR 1, involved in pre-mRNA splicing, is essential for megagametogenesis and embryogenesis in Arabidopsis. J Integr Plant Biol 2009; 51:261-71; PMID:19261069; http://dx.doi.org/10.1111/j.1744-7909.2008.00783.x
19. de la Fuente van Bentem S, Anrather D, Roitinger E, Djamei A, Hufnagl T, Barta A, Csaszar E, Dohnal I, Lecourieux D, Hirt H. Phosphoproteomics reveals extensive in vivo phosphorylation of Arabidopsis proteins involved in RNA metabolism. Nucleic Acids Res 2006; 34:3267-78; PMID:16807317; http://dx.doi.org/10.1093/nar/gkl429
20. de la Fuente van Bentem S, Anrather D, Dohnal I, Roitinger E, Csaszar E, Joore J, Buijnink J, Carreri A, Forzani C, Lorkovic ZJ, et al. Site-specific phosphorylation profiling of Arabidopsis proteins by mass spectrometry and peptide chip analysis. J Proteome Res 2008; 7:2458-70; PMID:18433157; http://dx.doi.org/10.1021/pr8000173
21. Palma K, Zhao Q, Cheng YT, Bi D, Monaghan J, Cheng W, Zhang Y, Li X. Regulation of plant innate immunity by three proteins in a complex conserved across the plant and animal kingdoms. Genes Dev 2007; 21:1484-93; PMID:17575050; http://dx.doi.org/10.1101/gad.1559607
22. Ausin I, Greenberg MV, Li CF, Jacobsen SE. The splicing factor SR45 affects the RNA-directed DNA methylation pathway in Arabidopsis. Epigenetics: official journal of the DNA Methylation Society 2012; 7:29-33
23. Dumesic PA, Natarajan P, Chen C, Drinnenberg IA, Schiller BJ, Thompson J, Moresco JJ, Yates JR 3rd, Bartel DP, Madhani HD. Stalled spliceosomes are a signal for RNAi-mediated genome defense. Cell 2013; 152:957-68; PMID:23415457; http://dx.doi.org/10.1016/j.cell.2013.01.046
24. Livak KJ, Schmittgen TD. Analysis of relative gene expression data using real-time quantitative PCR and the 2(-Delta Delta C(T)) Method. Methods 2001; 25:402-8; PMID:11846609; http://dx.doi.org/10.1006/meth.2001.1262
25. Bent AF. Arabidopsis in planta transformation. Uses, mechanisms, and prospects for transformation of other species. Plant Physiol 2000; 124:1540-7; PMID:11115872; http://dx.doi.org/10.1104/pp.124.4.1540
26. Cooper B, Eckert D, Andon NL, Yates JR, Haynes PA. Investigative proteomics: identification of an unknown plant virus from infected plants using mass spectrometry. J Am Soc Mass Spectrom 2003; 14:736-41; PMID:12837595; http://dx.doi.org/10.1016/S1044-0305(03)00125-9
27. Perkins DN, Pappin DJ, Creasy DM, Cottrell JS. Probability-based protein identification by searching sequence databases using mass spectrometry data. Electrophoresis 1999; 20:3551-67; PMID:10612281; http://dx.doi.org/10.1002/(SICI)1522-2683(19991201)20:18<3551::AID-ELPS3551>3.0.CO;2-2
28. Makarov A, Denisov E, Kholomeev A, Balschun W, Lange O, Strupat K, Horning S. Performance evaluation of a hybrid linear ion trap/orbitrap mass spectrometer. Anal Chem 2006; 78:2113-20; PMID:16579588; http://dx.doi.org/10.1021/ac0518811
29. Olsen JV, de Godoy LM, Li G, Macek B, Mortensen P, Pesch R, Makarov A, Lange O, Horning S, Mann M. Parts per million mass accuracy on an Orbitrap mass spectrometer via lock mass injection into a C-trap. Mol Cell Proteomics 2005; 4:2010-21; PMID:16249172; http://dx.doi.org/10.1074/mcp.T500030-MCP200
30. Beausoleil SA, Jedrychowski M, Schwartz D, Elias JE, Villén J, Li J, Cohn MA, Cantley LC, Gygi SP. Large-scale characterization of HeLa cell nuclear phosphoproteins. Proc Natl Acad Sci U S A 2004; 101:12130-5; PMID:15302935; http://dx.doi.org/10.1073/pnas.0404720101